International Journal of Nanomedicine

Dovepress
Taylor & Francis Group

Open Access Full Text Article

ORIGINAL RESEARCH

Transferrin and Borneol-Enhanced Liposomes for Targeted Rapamycin Delivery in TBI

Shihong Cai[1,2,*], Zhongwen Yuan[1,*], Yanfang Chen[3], Mingjie Gong[1], Jianqi Lai[1], Pengke Yan[1], Zhengrong Mei[1]

[1]Department of Pharmacy, Guangdong Provincial Key Laboratory of Major Obstetric Diseases, Guangdong Provincial Clinical Research Center for Obstetrics and Gynecology, The Third Affiliated Hospital, Guangzhou Medical University, Guangzhou, People's Republic of China; [2]Zhanjiang Healthcare Security Service Management Center, Zhanjiang, People's Republic of China; [3]Department of Pharmacy, Guangzhou Eighth People's Hospital, Guangzhou Medical University, Guangzhou, People's Republic of China

*These authors contributed equally to this work

Correspondence: Pengke Yan; Zhengrong Mei, Email gysyypk@126.com; meizhengrong@126.com

Background: The therapeutic potential of rapamycin (RAPA) for traumatic brain injury (TBI) is limited by its low bioavailability and poor penetration across the blood-brain barrier (BBB). We developed transferrin-modified rapamycin and borneol co-delivery liposomes (TF-RAPA/BO-LIP) to overcome these barriers, aiming to enhance both drug delivery to the brain and the treatment efficacy.

Methods: We employed the emulsion-solvent evaporation method to prepare TF-RAPA/BO-LIP and characterized their particle size, zeta potential, morphology, stability, and encapsulation efficiency. Pharmacokinetic studies were conducted in SD rats, and drug concentration was analyzed using LC-MS/MS. The brain-targeting capability and therapeutic efficacy were evaluated through in vitro cellular uptake studies, and in vivo in a TBI mouse model using both neurological and cognitive assessments.

Results: TF-RAPA/BO-LIP displayed optimal characteristics (95 nm particle size, >90% encapsulation efficiency) and demonstrated enhanced stability. Pharmacokinetic analyses revealed reduced drug clearance and increased drug concentration-time curve area, indicating improved systemic and brain-specific drug bioavailability. Notably, TF-RAPA/BO-LIP achieved significantly higher RAPA accumulation in the brain tissue. Importantly, treatment with TF-RAPA/BO-LIP significantly ameliorated neurological deficits and improved spatial memory in TBI mice, as evidenced by behavioral tests.

Conclusion: Our study highlights TF-RAPA/BO-LIP as a promising strategy for delivering RAPA across the BBB, substantially enhancing its therapeutic efficacy for TBI. This novel liposomal system not only improves RAPA bioavailability but also offers significant neuroprotection, potentially transforming the clinical management of TBI.

Keywords: traumatic brain injury, rapamycin, ferroptosis, liposomes

Introduction

Traumatic brain injury (TBI) is a significant neurological disorder resulting from closed or penetrating brain injuries induced by external forces. It represents a major cause of disability and mortality, inflicting substantial psychological and economic burdens on patients, families, and healthcare systems globally.[1–3] TBI is typically categorized into primary injuries, which are the immediate result of the initial impact, and secondary injuries, which evolve over time post-trauma.[4,5] Currently, the main treatments for TBI are removal of hematomas and repair of severe skull fractures, as well as prevention and treatment of complications, which including hyperthermia, hyponatremia and seizures.[6–8] Many of the current therapies will have some positive impact on the prognosis of TBI patients, however, the therapeutic effects are still very limited, and it is not yet to reverse the primary injury. Therefore, the main way to repair central nervous system (CNS) damage is to mitigate the damage caused by secondary injury. However, there are no neuroprotective agents that can significantly alleviate neurological damage, and further experiments are needed to explore suitable drugs for

Received: 29 July 2024
Accepted: 28 February 2025
Published: 11 April 2025

neurological impairment after TBI.[9–11] Current therapeutic strategies are limited, and the delivery of drugs like rapamycin (RAPA) is particularly challenging due to its poor blood-brain barrier (BBB) permeability.[12]

RAPA is recognized for its extensive biological activities, including immunosuppressive, antiproliferative, antiangiogenic, antifungal, and anti-inflammatory properties. Specifically, RAPA has shown potential in ameliorating CNS injuries by inhibiting astrocyte proliferation and neuroglial scar formation.[13] However, ts therapeutic application is severely limited by poor water solubility and high molecular weight, which contribute to low bioavailability and restricted BBB penetration when administered orally.[14,15] After the RAPA is absorbed into the blood circulation, most of the drug is distributed in red blood cells and only a small amount of the drug is distributed in plasma, and it is difficult to cross the BBB, so the drug efficacy is low, which limits the application of RAPA in neurological diseases.[16,17] Advancements in nanotechnology have spurred the development of nanocarrier drug delivery systems (NDDS), which encapsulate therapeutics like RAPA to facilitate BBB crossing.[18–20]

Liposomes are spherical vesicles composed of cholesterol and amphiphilic phospholipids and are a promising drug delivery system.[21] Liposomes have various properties such as excellent biocompatibility, low clearance, safety, and can be aggregated at the site of inflammation, infection, and tumor lesions, therefore, liposomes can be used for delivery of drugs.[22–28] In addition, liposomes can be surface-modified with proteins, antibodies, aptamers, or peptides to acquire targeting capabilities.Transferrin (Tf) is a single-chain glycoprotein that can bind specifically to Transferrin receptor (TfR).[29–32] TfR is a specific receptor present on the cell surface, which is over-expressed in brain capillary endothelial cells.Therefore, liposomes can be surface-modified with Tf to acquire brain-targeting ability.[33–35] By modifying liposomes with transferrin, our approach leverages receptor-mediated endocytosis to facilitate enhanced crossing of the BBB. Transferrin acts as a ligand that binds to its corresponding receptors on the BBB, promoting the uptake of the entire liposome into the brain endothelial cells.[35–37] However, existing systems often fail to achieve desired therapeutic concentrations in the brain, necessitating frequent dosing or higher doses, which could lead to systemic toxicity.[37–40]

Borneol(BO) is obtained by distillation and recrystallizing from the leaves and stems of Blumea balsamifera DC or Cinnamomum camphora Presl. BO is a penetration enhancer that assists other compounds or delivery systems to penetrate physiological barriers.[41–43] BO is a bicyclic monoterpene that has been used as an adjuvant in the formulation of traditional Chinese medicine for the treatment of CNS diseases. As a Permeability Enhancer, borneol serves to temporarily alter the tight junctions of the BBB, increasing its permeability, thus improving the brain delivery of drugs and enhancing the distribution of drugs in the BBB to improve bioavailability.[44–48] Therefore, we have developed a novel liposomal delivery system that incorporates both transferrin and borneol. This system is designed to enhance the cerebral delivery of rapamycin by exploiting transferrin receptors, which are overexpressed on the BBB, and by utilizing borneol to transiently disrupt the BBB, thereby allowing larger molecules to pass through. This dual-action strategy synergistically improves the transport of rapamycin into the brain, potentially increasing its therapeutic concentrations at the site of injury.

In the study, we developed Tf-modified RAPA and BO co-delivery liposomes (TF-RAPA/BO-LIP) to enhance drug distribution within the brain and extend drug circulation time (Figure 1). We evaluated the therapeutic efficacy of TF-RAPA/BO-LIP in a TBI mouse model and found that it significantly improved the therapeutic outcomes of RAPA on neurological impairments post-TBI. These findings suggest that TF-RAPA/BO-LIP represents a promising new therapeutic strategy for TBI treatment.

Materials and Methods

Materials, Cells and Animals

Rapamycin were purchased from Widely Chemical Co., Ltd (Wuhan, China). Phospholipid and sodium cholesterol sulfate were purchased from Avito Biotech Co., Ltd (Shanghai, China). Coumarin 6 was purchased from TCI (Japan). DIR was supplied by the Meilun Biotechnology Co., Ltd. (Dalian, China). Penicillin–streptomycin and DMEM, trypsin EDTA and FBS were purchased from Gibco Life Technologies (AG, USA). DSPE-PEG2000-Tf were obtained from Xi'an Ruixi Biological Technology Co. Ltd (Xi'an, China). Roxithromycin was purchased from Meilun Biotechnology Co., Ltd. (Dalian, China). Total Superoxide Dismutase Assay Kit with WST-8 and a Lipid Peroxidation MDA Assay kit were purchased from Beyotime Biotechnology Co., Ltd (Shanghai, China). GPX4 (lipid hydroperoxidase glutathione

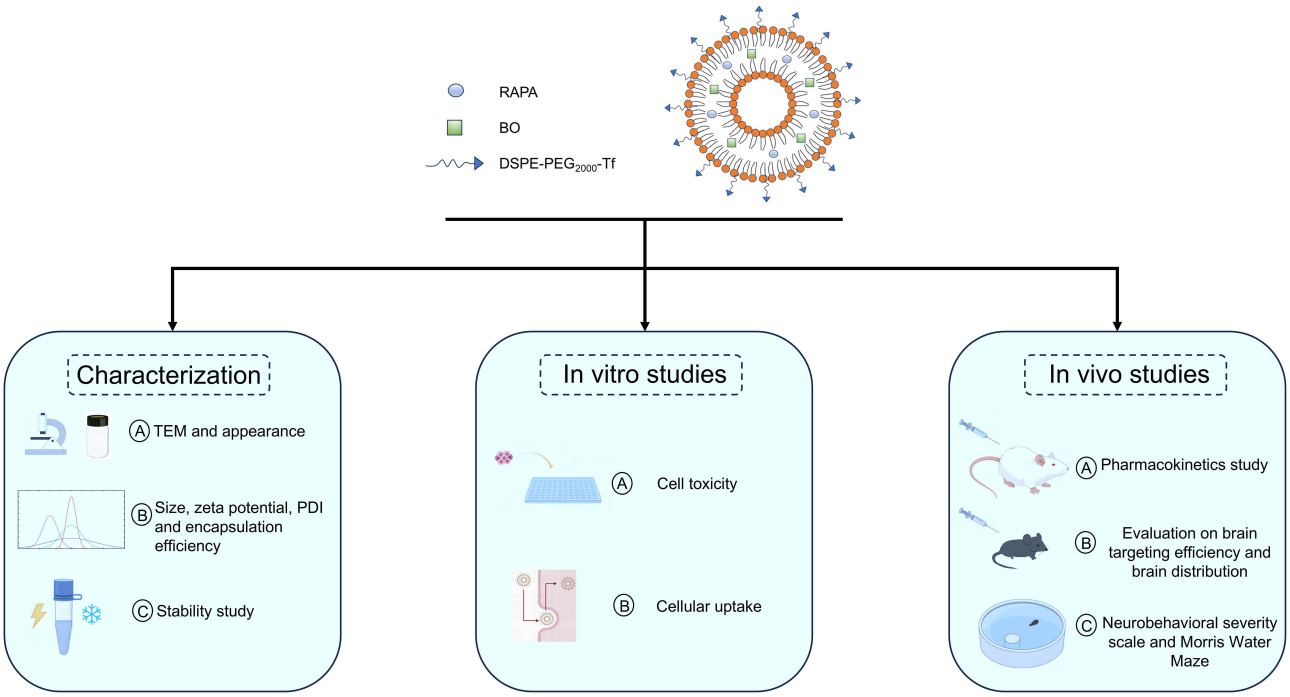

Figure 1 Schematic illustration displaying the study of transferrin modified rapamycin and borneol co-delivery liposome.

peroxidase 4) antibody was obtained by the Abcam Co., Ltd. (Shanghai, China). SLC7A11 (xCT, the functional component of system Xc-), SLC3A2 (4F2hc, the functional component of system Xc-), FTH1 (ferritin heavy chain) and DMT1 (divalent metal transporter) antibodies were purchased from Cell Signaling Technology Co., Ltd (Shanghai, China). All other chemicals used were of analytical grade.

Human glioma cell line U87 cells were provided by Zhujiang Hospital of Southern Medical University (Guangzhou, China). U87 cells were cultured in DMEM medium supplemented with 10% FBS and 1% penicillin-streptomycin, and were incubated at 37°C in a humidified atmosphere of 5% CO_2.

Sprague-Dawley rats (male, 220–250 g) and C57BL/6J mice (male, 8 weeks old) were purchased from the Guangdong Medical Laboratory Animal Center. All animals were acclimated and maintained in animal facilities for 7 days with temperatures of 21–27°C, relative humidity of 50–60% and a light/dark cycle of 12/12 h. The animals were fasted for 12 h prior to experiment, with water ad libitum.All procedures were performed according to the guidelines for the Care and Use of Laboratory Animals of Guangzhou Medical University, and the experiments were approved by the Third Affiliated Hospital of Guangzhou Medical University Institutional Animal Care and Use Committee ([2023]-147).

Preparation of Tf-Modified RAPA and BO Co-Loaded Liposomes

The preparation of transferrin-modified rapamycin and borneol co-delivery liposomes (Tf-RAPA/BO-LIP) involved an emulsion-solvent evaporation and sonication method. This process was utilized to create three nanoparticle formulations: RAPA-LIP, Tf-RAPA-LIP, and Tf-RAPA/BO-LIP. Briefly, the oil phase (OP) comprised 10 mg of RAPA, 15mg of BO, 136 mg of phospholipid, and 2.5% DSPE-PEG_{2000}-Tf (DSPE-PEG2000-Tf/phospholipid, w/w). These components were dissolved in 2 mL dichloromethane (DCM). 24 mg cholesteryl sodium sulfate (CHOS) was ultrasonically dispersed in the aqueous phase (AP, 20 mL PBS).

Firstly, the OP was mixed with the AP and sonicated (JY92IID ultrasonic processor, Ningbo Xinzhi Biotechnology Co., Ltd, China) at 200 W for 5 min in an ice-water bath to obtain an emulsion, which was then placed in a 45 °C water bath to volatilize the organic solvent. Then, it was sonicated in an ice-water bath at 100 W for 5 min. The unencapsulated RAPA was filtered using a 0.22 μm cellulose nitrate membrane. The TF-RAPA/BO-LIP were freeze-dried using an LGJ-10C freeze dryer (Beijing Sihuan Furuike Instrument Technology Development Co., Ltd, China) with 8% (w/v) sucrose

https://doi.org/10.2147/IJN.S489165

solution as the freeze-drying protective additive. RBL were prepared by the same composition and method as TF-RAPA /BO-LIP without the addition of DSPE-PEG2000-Tf. RAPA-LIP was prepared through the same process as TF-RAPA /BO-LIP without addition of DSPE-PEG_{2000}-Tf and Borneol. Liposomes for cellular uptake studies were produced by replacing RAPA with coumarin-6 (C6) according to the same procedure (C6-LIP, Tf-C6-LIP, and Tf-C6/BO-LIP). DIR-loaded liposomes (DIR-LIP, DIR/BO-LIP, and Tf-DIR/BO-LIP) for the NIR fluorescence imaging studies were produced using a similar process.

Characterization of RAPA Liposomes

Particle Size, Zeta Potential, and Morphology

The particle size, polydispersity index and zeta potential values of liposomes were determined using dynamic laser light scattering (DLS) with a Malvern Zetasizer Nano ZS instrument at 25°C (ZEN3500, Nano ZS Instruments, Worcestershire, UK). The morphology of liposomes were explored using transmission electron microscopy (TEM).

Measurement of Encapsulation Efficiency (EE) of RAPA Liposomes

To measure EE% of liposomes, liposomes were obtained by microporous membrane filtration (0.22 μm) and centrifugation (14,000 rpm, 15 min, 4°C). 100 μL of the upper liposomes solution was demulsified by adding 900 μL of methanol and centrifuged at 14,000 rpm for 15 min at 4°C. 10 μL of supernatant was injected into the High Performance Liquid Chromatography (HPLC) for analysis the amount. The EE% was calculated using the following equation:

$$EE\% = (We/Wt)^{*}100\%$$

We represents amount of RAPA encapsulated in liposomes, and Wt represents the total amount of RAPA.

Chromatographic conditions used for RAPA included: C18 analytical column (Diamonsil® C18 Column, 4.6 mm×250 mm, 5 μm, Dikma Technologies Inc., China); mobile phase: methanol/acetonitrile/water (43/40/17, v/v/v); running time: 20 min; flow rate: 1.0 mL/min; injection volume: 10 μL; column temperature: 40 °C; UV detection wavelength: 278 nm.

Stability of Liposomes in Vitro

The stability of liposomes was executed by determining the amount of drug or EE% and particle size. The liposomes were mixed with PBS solution (pH 7.4) or 50% plasma (1:1, v/v) and incubated in a water bath at 37°C with gentle shaking. At predetermined times (0, 1, 2, 4, 8, 12, and 24 h), samples were taken to detect the drug amount and particle size. Liposomes were stored at 4°C and samples were taken at 0, 7, 15, 21, and 30 days for analysis of drug content and particle size.

Brain Targeting Study and Cellular Uptake in Vitro

Flow cytometry (FCM) and laser confocal scanning microscopy (LSCM, Nikon, Japan) were employed to study the uptake of fluorescently-labeled C6-loaded liposomes (C6-LIP, C6/BO-LIP, and Tf-C6/BO-LIP) in U87 cells. U87 cells were inoculated into 6-well plates (1×10^5 cells/well) and incubated for 24 h. The medium was then replaced by fresh medium containing C6 solution, C6-LIP, C6/BO-LIP, Tf-C6/BO-LIP (C6= 5 μg/mL) and incubated for 2 h.Then, the medium was removed and cells were fixed with 4% paraformaldehyde for 15 min, stained with DAPI (2.5 ug/mL) and washed three times with PBS. The cellular uptake was determined by LSCM and FCM.

Cell Viability

HT22 cells were seeded in 96-well plates at a density of 5×10^4 cells. After incubation for 24h, the culture medium was replaced with the free RAPA solution, RAPA-LIP, TF-RAPA-LIP, and TF-RAPA/BO-LIP, respectively, incubation for 24h. The cell viability was detected by MTT assay kit (Solarbio, Beijing, China). The preparation were replaced with 100 μL of MTT solution (5 mg/mL) prepared with DMEM medium for 4 h. Then, MTT was removed, and 100 μL of DMSO was added to each well to dissolve the formazan crystals. Absorbance values were measured at 490 nm using

a microplate reader (Bio-Rad Model 680, UK). The drug concentration at which the growth of 50% of the cells was inhibited (IC50) was assayed by curve fitting of cell viability data compared with that of the control group.

Pharmacokinetics Study

Twenty-four healthy SD rats were randomly divided into four groups (n=6). The different RAPA formulations, namely the free RAPA solution, RAPA-LIP, TF-RAPA-LIP, and TF-RAPA/BO-LIP, were injected into the rats via tail vein at a dose of 3 mg/kg. Blood samples (0.5 mL) were collected in heparinized tubes from orbital veins of rats at predetermined time points, namely 0.083, 0.1667, 0.25, 0.3333, 0.5, 1, 2, 4, 8, 12, and 24 h.

The concentration of RAPA in blood was determined using liquid chromatography-mass spectrometry (LC-MS/MS) apparatus (Triple QuadTM 4500MD, SCIEX, USA) equipped with an electrospray ionization (ESI) source. Quantification was operated in the positive ESI mode [ESI (+)]. A C18 analytical column (ZORBAX SB-C18, 2.1×100 mm, 3.5 μm, Agilent Technologies Inc., USA) was used for detection. The mobile phase consisted of phase A (0.1% formic acid) and phase B (methanol/acetonitrile (90/10, v/v)) The gradient elution program with a flow rate at 0.7 mL/min was as follows: 0–0.3 min, 20% phase B; 0.3–1.2 min, 70% phase B; 1.2–3.1 min, 95% phase B; 3.1–5.5 min, 20% phase B. The run time was 5.5 min. The temperature for the auto-sampler and column was 4°C and 40°C, respectively.

MS parameters: acquisition mode: multiple reaction monitoring (MRM); declustering potential(DP): 120 V; entrance potential (EP): 10 V; collision energy (CE): 24 V; collision cell exit potential (CXP): 6 V; transitions (m/z): RAPA (931.7→864.5) ROX (837.6→679.7); curtain gas (CUR): 35 psi; collision-activated dissociation (CAD): 9 units; ion spray voltage(IS): 5500 V; nebulizer gas (GS1): 50 psi; heater gas (GS2): 55 psi; ion source house temperature (TEM): 500°C. The LC-MS/MS system control and data analysis were performed using Analyst MD software (Version 1.6.3, SCIEX, USA)). The pharmacokinetic parameters were analyzed using a two-compartmental analysis model with the Drug and Statistics 2.0 (DAS2.0) software.

TBI Model

C57BL/6J mice underwent a modified repetitive mild closed head injury protocol to induce traumatic brain injury (TBI).[13] The mice were anesthetized with ether and positioned prone position on a stereotaxic apparatus with their heads aligned under a metal hollow guide tube. A 54-gram metal weight was dropped from a height of 28 inches through the tube to impact the bregma of the mouse skull.

Over a nine-day period, all mice except those in the sham-operated group (which received only anesthesia without injury) sustained seven impacts to the head over a nine-day period, specifically, daily from days 1 to 5, with a pause on days 6 and 7, followed by additional impacts on days 8 and 9. Each session concluded with the mice being placed in fresh air to allow them to awaken and recuperate.

RAPA Distribution in the Brains of TBI Mice

TBI mice were randomly divided into four groups (n=6). Different RAPA preparation, namely free RAPA solution, RAPA-LIP, TF-RAPA-LIP, and TF-RAPA/BO-LIP were injected into the mice via tail vein at a dose of 3 mg/kg. The mice were sacrificed at 1h, 3h, 6h and 24h after injection. The brain tissues of mice were obtained and washed with PBS to remove the blood attached to the organs, and weighed. The concentration of RAPA in brain tissue was determined by LC-MS/MS as described previously.

Imaging in TBI Mice

TBI mice were used to evaluate the distribution of Tf-modified liposomes in vivo. TBI mice were randomly divided into four groups (n=5). Different DIR formulations, namely the free DIR, DL, TDL, and TDBL were injected into the mice via tail vein at a dose of 0.8 mg/kg. The mice were then anesthetized with 4% chloral hydrate, and fluorescent and normal images of the mice were captured using an in vivo imaging system at 1,3,6, and 24 hours. Subsequently, the mice were sacrificed and the brain were removed at 24h after injection. In vivo imaging system was used to observe fluorescence of brain.

Neurobehavioral Severity Scale (NSS)

At 24 h after the end of the TBI modeling, the Revised Neurobehavioral Severity Scale (NSS-R)[49] was used to assess the degree of neurological impairment in mice, which mainly tested 10 aspects including balance, landing, tail lifting reflexes and so on.The total score ranges from zero to ten, with a higher score indicating more serious neurological function impairment.

Morris Water Maze (MWM)

TBI mice were randomly divided into four groups (n=6) and treated with different RAPA formulations: free RAPA solution, RAPA-LIP, TF-RAPA-LIP, and TF-RAPA/BO-LIP administered via tail vein at a dose of 3 mg/kg/d. After 25 days of treatment, the MWM test was performed to evaluate the effect of TF-RAPA/BO-LIP on the learning and memory capacity of the TBI mice. The apparatus included a white circular constant temperature pool, with a diameter of 120 cm and a depth of 29 cm, filled with water at 25 °C. The pool was equally divided into four quadrants (north, south, east, and west) and featured a submerged escape platform placed 1 cm below the water surface in a designated target quadrant. Mice were randomly placed at different starting points facing the pool wall and allowed to search for the platform for 60 seconds. If a mouse found the platform within this time, it remained there for 15 seconds before being removed. If it did not find the platform, it was guided to it and allowed to stay for 15 seconds. This training occurred four times daily over five consecutive days, with the time taken to find the platform recorded as the escape latency. On the sixth day, the platform was removed to evaluate memory retention; mice were observed for their ability to locate the former platform area, with their path and latency tracked. All images and data were recorded by the data collection and analysis system (Chengdu Taimeng Technology Co.,Ltd., Chengdu, China).

The Protective Effect of RAPA in TBI Mice

All mice were divided into three groups (n=6), namely the Sham group, TBI group, RAPA group. The RAPA-treated TBI mice were injected into the mice via tail vein at a dose of 3 mg/kg/d. The mice in the Sham and TBI groups were treated with PBS. After 25 days of treatment with different formulations, each group of mice was sacrificed to evaluate the therapeutic effects. According to the manufacturer's instructions, the levels of SOD activity and MDA were detected by a Total Superoxide Dismutase Assay Kit with WST-8 and a Lipid Peroxidation MDA Assay kit. GXP4, SLC7A11, SLC3A2, FTH1 and DMT1 proteins expression were tested by Western blot analysis.

Statistical Analysis

The results were expressed as the mean ± standard deviation (SD). All data were analyzed using one-way analysis of variance (ANOVA) in GraphPad Prism 9.0 statistical software (La Jolla, CA, USA). A value of P less than 0.05 were considered to be statistically significant.

Results and Discussion

Characterization Liposomes and Stability Evaluation

The prepared RAPA-loaded liposomes exhibited a pale blue opalescent liquids with a translucent appearance and presented an appropriate particle sizes (Figure 2A and B). The particle size is a critical determinant for BBB penetration. Studies indicate that nanoparticles larger than 200 nm are nearly impermeable across the BBB,[50,51] and with those smaller than 5 nm rapidly cleared by renal filtration.[52] Optimal nanoparticles for BBB delivery should range between 10–100 nm in diameter. Through ultrasonication, we achieved a uniform particle size distribution with a reduced polydispersity index (PDI), optimizing liposome uptake efficiency.

The particle sizes, PDI, zeta potential, and encapsulation efficiency (EE%) of the liposomes are summarized in Table 1. The particle sizes were as follows: RAPA-LIP (size: 78.87±0.86 nm, PDI = 0.150±0.006), TF-RAPA-LIP (size: 84.22±0.62 nm, PDI = 0.135±0.004) and TF-RAPA/BO-LIP (size: 90.76±0.55 nm, PDI = 0.136±0.008). The slight increase in size for TF-RAPA/BO-LIP suggests the successful incorporation of DSPE-PEG2000-Tf into the lipid bilayer. The EE% across the formulations was impressively high (>90%), indicating efficient drug loading: RAPA-LIP (93.39±1.20%), TF-RAPA-LIP

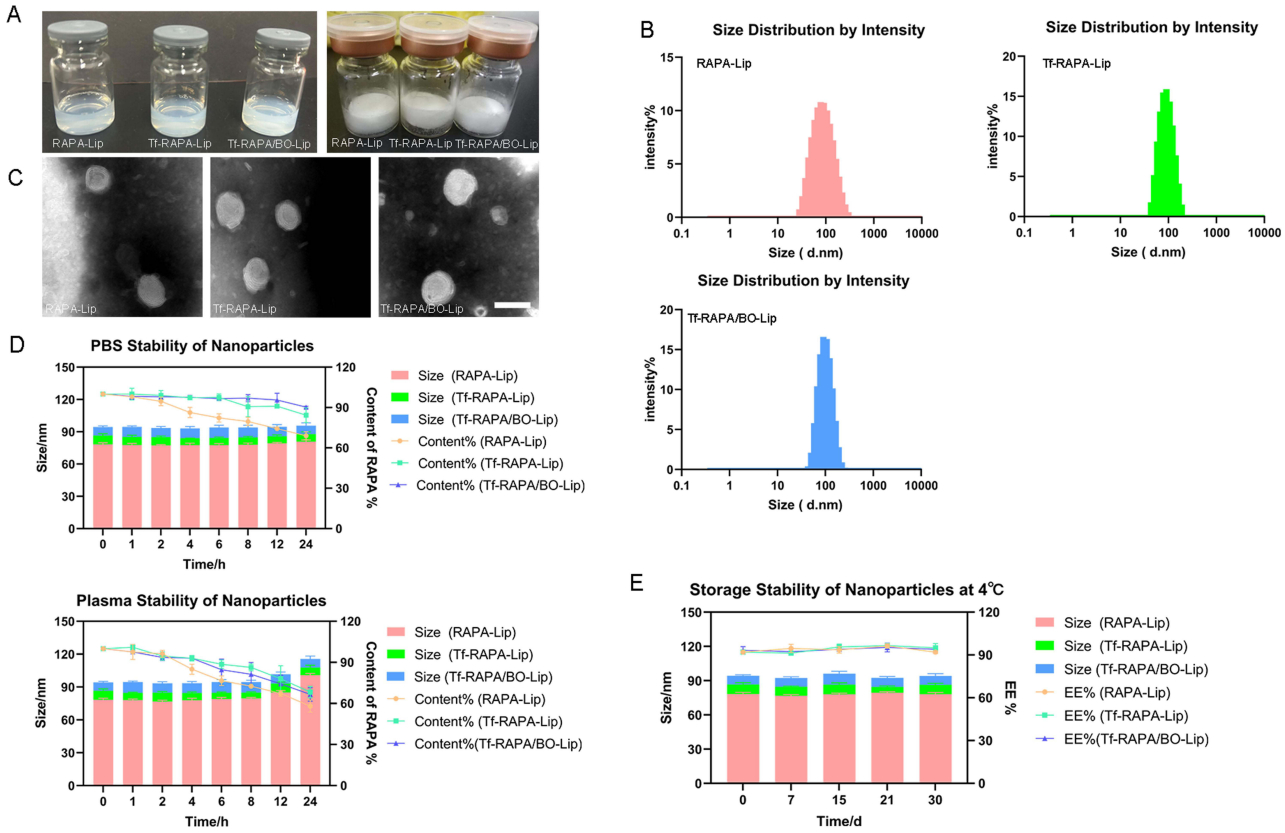

Figure 2 Characterization and stability evaluation of liposomes. (**A**) Liposome samples. (**B**) TEM images of liposomes, scale bar=50 nm. (**C**) Particle sizes of liposomes. (**D**) Stability of liposomes in PBS or 50% plasma at 37°C. (**E**) Stability of liposomes at 4°C after 30-days storage.

(94.44±1.89%), and TF-RAPA/BO-LIP (92.12±1.03%). Zeta potential measurements indicated good colloidal stability, with RAPA-LIP at −48.30±2.86 mV, TF-RAPA-LIP at −43.83±3.06 mV, and TF-RAPA/BO-LIP at −41.39±3.75 mV, due in part to the negatively charged cholesteryl sodium sulfate (CHOS).When the zeta potential of the liposomes is higher than 30 mV, the liposomes repel each other, avoiding particle aggregation and thus maintaining the long-term stability of the liposomes. TEM analysis (Figure 2C) confirmed that the liposomes were regular and spherical, with an approximate diameter of 100 nm.

Plasma stability experiments revealed a slight increase in liposome size over time, likely due to protein adsorption causing aggregation. However, there was no significant change in size or drug content within 24 hours, indicating good plasma stability (Figure 2D). When incubated in PBS (pH 7.4) at 37 °C for 24 h, the liposomes showed stable size and drug content, further supporting their robustness in physiological conditions.Long-term storage stability was also assessed, with liposomes stored at 4°C for 30 days. Both size and EE% remained within acceptable ranges during this period, demonstrating excellent storage stability (Figure 2E).

Overall, our characterization and stability studies confirm that the RAPA-loaded liposomes, particularly the Tf-modified and borneol co-delivery formulations, are well-suited for further in vitro and in vivo evaluations. Their size, stability, and high drug loading efficiency make them promising candidates for effective drug delivery across the BBB,

Table 1 Characteristics of Various LPs. Data are Presented as the Mean ± SD (n = 3)

Preparations	Size (nm)	PDI	Zeta Potential (mV)	EE (%)
RAPA-LIP	78.87±0.86	0.150±0.006	−48.30±2.86	93.39±1.20
TF-RAPA-LIP	84.22±0.62	0.135±0.004	−43.83±3.06	94.44±1.89
TF-RAPA/BO-LIP	90.76±0.55	0.136±0.008	−41.39±3.75	92.12±1.03

https://doi.org/10.2147/IJN.S489165

potentially enhancing therapeutic outcomes for TBI. These findings substantiate the potential application of these nanoformulations in clinical studies targeting neurological conditions.

Cellular Uptake and Cell Viability

The internalization of liposomes by U87 cells was assessed using LSCM and FCM, utilizing coumarin 6 (C6) as a fluorescent probe instead of RAPA to assess the specific targeting ability of Tf-modified formulations. LSCM images (Figure 3A) displayed a higher cellular uptake of C6- loaded liposomes compared to free C6. Notably, the uptake of Tf-C6-Lip and Tf-C6/BO-Lip by U87 cells was superior to that of C6-Lip after a 2-hour incubation at 37°C. Quantitative analysis by FCM (Figure 3B) further confirmed that Tf-modified liposomes (Tf-C6-LIP and Tf-C6/BO-LIP) showed enhanced fluorescence intensity compared to C6-Lip, indicating higher uptake. These results validate the successful construction of Tf-modified and borneol co-delivery liposomes with significant homologous targeting capacity, underscoring their potential for brain-targeted delivery.

The cytotoxic effects of the liposomal formulations were assessed using the MTT assay on HT22 cells. As shown in Figure 3C, all RAPA formulations demonstrated dose-dependent inhibition of HT22 cell growth. However, the IC50 values of the liposomal formulations were lower than that of the free RAPA solution, although without significant differences among the liposomes themselves. These findings suggest that the liposomal formulations are less toxic and

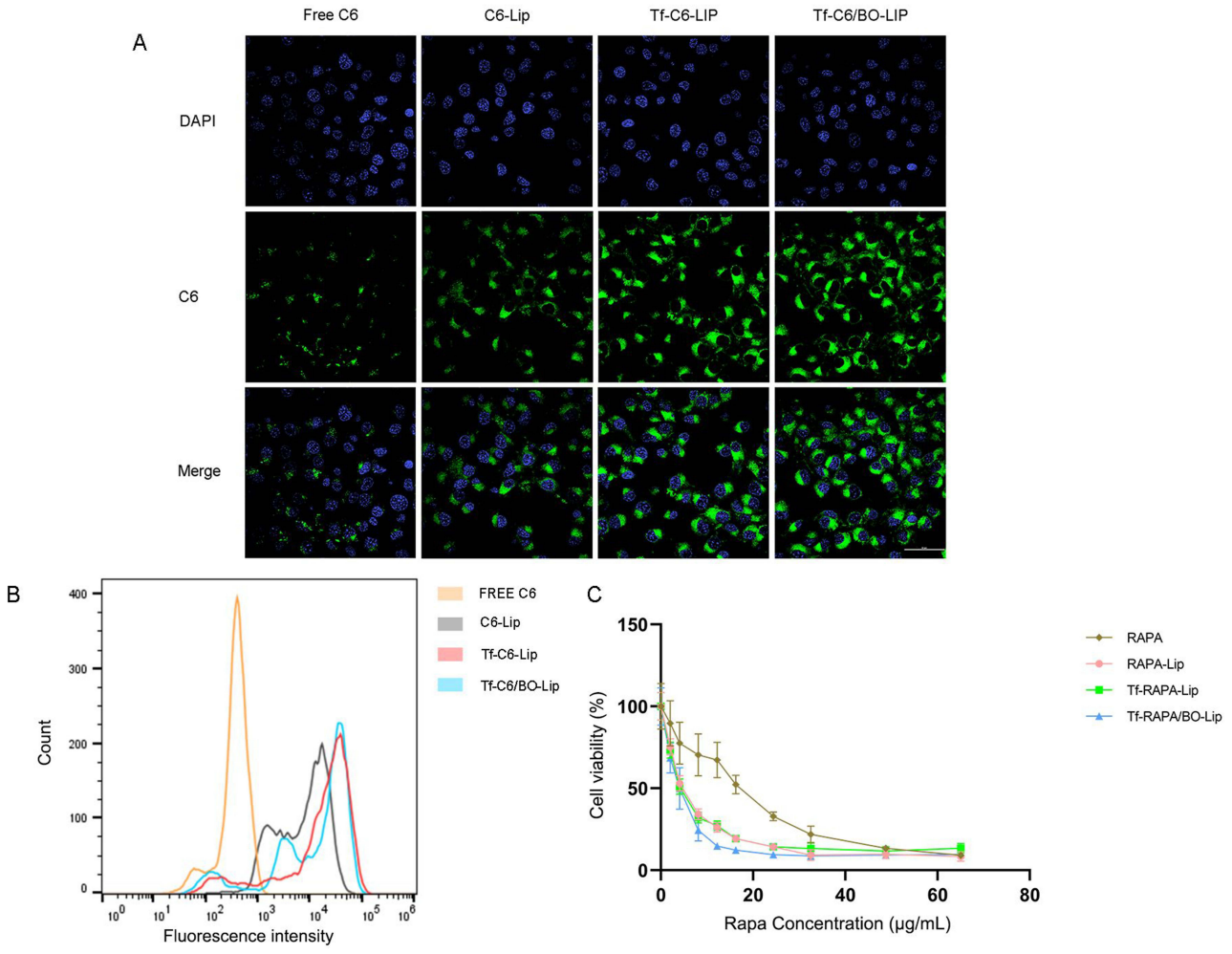

Figure 3 Cellular uptake and distribution after incubation with varying formulations, scale bar=50 μm. (**A**) LSCM fluorescence images of U87 cells after incubation with Free-C6, C6-LIP, Tf-C6-LIP, andTf-C6/BO-Lip for 2 h ([C6] = 5 μg/mL). (**B**) Cellular uptake of U87 cells treated with Free-C6, C6-LIP, Tf-C6-LIP, andTf-C6/BO-Lip for 2 h ([C6] = 5 μg/mL). (**C**) The cell viability of HT22 cells and after treatment of free RAPA solution, RAPA-Lip, Tf-RAPA-Lip and Tf-RAPA/BO-Lip for 24 hours.

safer for therapeutic use compared to the free drug, aligning with studies suggesting an optimal therapeutic concentration of RAPA around 2 nM for neuronal cells.[53]

Pharmacokinetics Analysis

The pharmacokinetic profiles following intravenous administration of various RAPA formulations were shown in Figure 4A, with pharmacokinetic parameters summarized in Table 2. Following administration, a rapid peak in blood drug concentration was observed, which then decreased gradually. The pharmacokinetic modeling matched a two-compartment model, indicating distinct distribution and elimination phases.

The clearance rates for free RAPA solution, RAPA-LIP, TF-RAPA-LIP and TF-RAPA/BO-LIP were 0.64±0.10, 0.39 ±0.10, 0.35±0.09, 0.37±0.10 L/h/kg, respectively. The clearance rate of free RAPA solution was significantly higher (1.6–1.8-fold) than that of liposomal formulations ($P<0.05$), underscoring the effectiveness of liposomes in reducing drug elimination from the bloodstream. Notably, the area under the curve value ($AUC_{0-\infty}$) for TF-RAPA-LIP and TF-RAPA /BO-LIP showed a 1.9-fold and 1.8-fold increase, respectively, compared to the free drug ($P<0.05$). Additionally, the mean retention time (MRT) of the liposomal formulation was 2.3–3.0-fold greater than that of the free RAPA solution, and the elimination half-life ($t_{1/2\beta}$) of the liposomal formulation was prolonged and 2.3–2.8-fold higher than that of the free RAPA solution. These pharmacokinetic results demonstrate that Tf-modified and borneol co-delivery liposomal

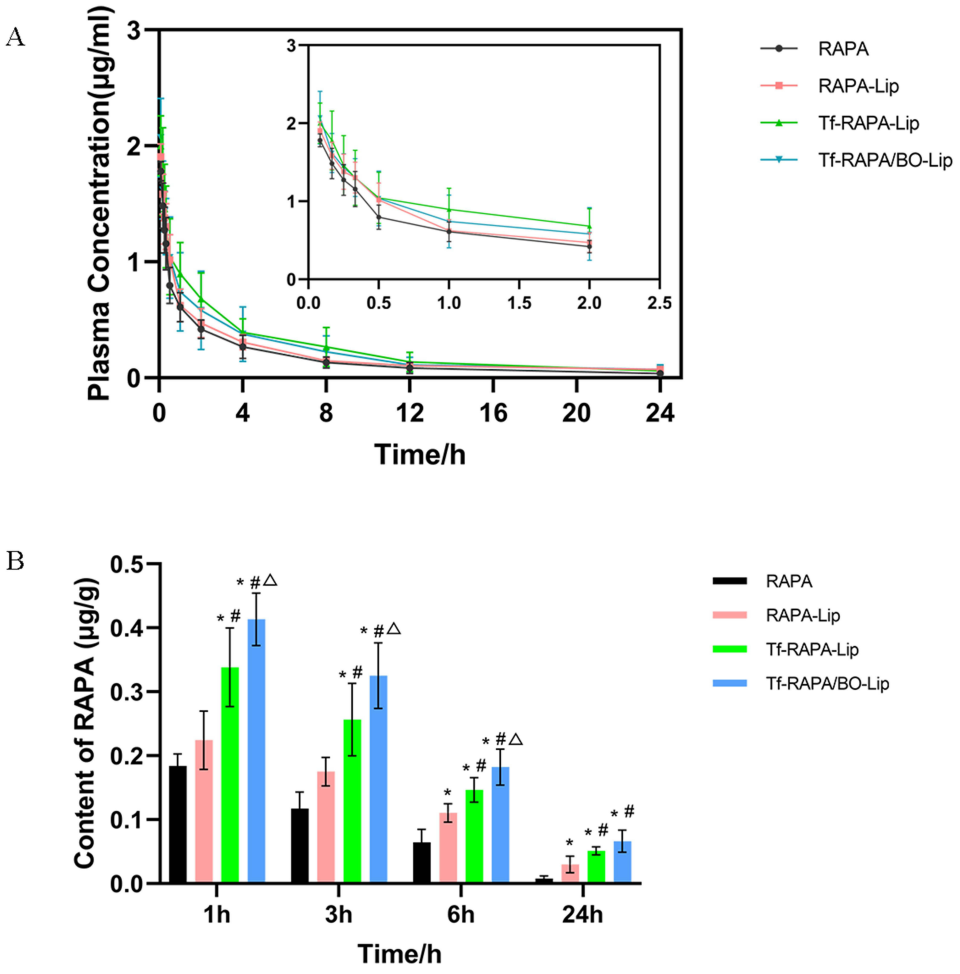

Figure 4 Plasma concentration-time curve of RAPA in SD rats and RAPA concentration in brain of the varying formulations at different time points. (**A**) Plasma concentration–time curve of RAPA pharmacokinetic (PK) profile in SD rats following intravenous administration of the varying formulations (3 mg/kg). (**B**) Drug concentration in brain of TBI mice of free RAPA solution, RAPA-Lip, Tf-RAPA-Lip and Tf-RAPA/BO-Lip groups at different time points. Data are presented as mean ± SD (n=6). RAPA compared with liposomes, $^{*}P<0.05$; RAPA-Lip compared with Tf-RAPA-Lip or Tf-RAPA/BO-Lip, $^{\#}P<0.05$; Tf-RAPA-Lip compared with Tf-RAPA/BO-Lip, $^{\triangle}P< 0.05$.

https://doi.org/10.2147/IJN.S489165

Table 2 Pharmacokinetic Parameters of RAPA Following Intravenous Administration of the Varying Formulations at the Dose of 3.0 mg/kg in SD Rats (Mean ± SD, n = 6)

Parameters	Unit	RAPA	RAPA-LIP	TF-RAPA-LIP	TF-RAPA/BO-LIP
t1/2α	h	0.90±0.42	0.99±0.30	1.45±0.71	1.05±0.96
t1/2β	h	12.18±3.91	27.86±15.50	31.41±17.38	33.70±13.34
K10	1/h	0.35±0.08	0.20±0.05	0.17±0.06*	0.25±0.19
K12	1/h	0.58±0.64	0.48±0.27	0.31±0.17	0.84±0.99
K21	1/h	0.19±0.16	0.11±0.03	0.12±0.10	0.19±0.26
CL	L/h/kg	0.64±0.10	0.39±0.10*	0.35±0.09*	0.37±0.10*
AUC0-∞	mg/L/h	4.76±0.78	8.04±2.12	8.95±2.43*	8.76±3.18*
MRT	h	10.40±2.69	29.88±21.20	27.47±16.81	30.93±13.78

Notes: liposomes compared with RAPA, *P<0.05.

formulations significantly enhance systemic exposure and prolong circulation time of RAPA, improving its bioavailability. The extended circulation and reduced clearance rates are indicative of the potential of these formulations to facilitate more effective drug delivery to the brain, highlighting their utility in improving therapeutic outcomes for conditions such as TBI.

Liposome Distribution in the Brain

Due to the integrity of the BBB, the nanodelivery system that penetrate the BBB have to enter the brain to better utilize the therapeutic effects of RAPA on neurological impairments. It has been reported that Tf-modified liposomes can transport drugs across the BBB.[38,39] To evaluate the efficacy of different RAPA formulations in crossing the BBB and delivering therapeutic effects, TBI mice were administered various formulations intravenously. The concentration of RAPA in brain tissues was quantitatively analyzed and presented in Figure 4B. Results indicated that at all predefined time points, the drug levels in the brain tissues of the Tf-modified liposome groups (TF-RAPA-LIP and TF-RAPA/BO-LIP) were consistently higher than those in the unmodified liposome group and significantly exceeded those in the free RAPA solution group. This enhanced delivery is attributed to the receptor-mediated endocytosis facilitated by Tf-modification, which supports homologous targeting. Notably, brain accumulation of TF-RAPA/BO-LIP was higher than that of TF-RAPA-LIP at 1h and 3h post-administration, suggesting that borneol enhances BBB penetration. In addition, the drug content in the brain of the free RAPA formulations group decreased rapidly after administration due to the rapid metabolism of RAPA. However, the drug content in the liposome group decreased slowly within 24h due to the sustained-release effect of liposomes.The slow decline in drug levels in liposome groups compared to the rapid decrease in the free RAPA solution group further underscores the sustained-release properties of the liposomal formulations, confirming their efficacy in targeted brain delivery.

Imaging of Liposomes in TBI Mice

To visually assess the brain-targeting capabilities of the liposomal formulations, DIR dye was used as a replacement for RAPA to track the distribution within the brains of TBI mice.Fluorescent imaging results (Figure 5A) showed minimal signal in the brain from free DIR post-injection. In contrast, significant fluorescence was observed in the brains of mice treated with DIR-LIP, Tf-DIR-LIP, and Tf-DIR/BO-LIP, with the latter two showing considerably stronger signals than DIR-LIP alone. This enhancement is due to the specific homologous targeting of Tf-modified liposomes, which facilitates BBB crossing through receptor-mediated endocytosis. Moreover, the stronger fluorescence signal from Tf-DIR/BO-LIP compared to Tf-DIR-LIP indicates that borneol further promotes BBB penetration, enhancing brain delivery capabilities. At 24h post-administration, brains were extracted from the mice and analyzed using a whole fluorescence imaging system to measure tissue-level accumulation. The imaging results (Figure 5B) revealed that the Tf-DIR/BO-LIP group displayed the most robust fluorescence signals, aligning with the in vivo fluorescence imaging data. These findings affirm that TF-RAPA/BO-LIP possesses superior BBB infiltrating ability and effective brain-targeting properties.On one hand, By modifying liposomes with transferrin, we enhance the uptake of rapamycin-loaded particles into the brain via receptor-mediated endocytosis. This

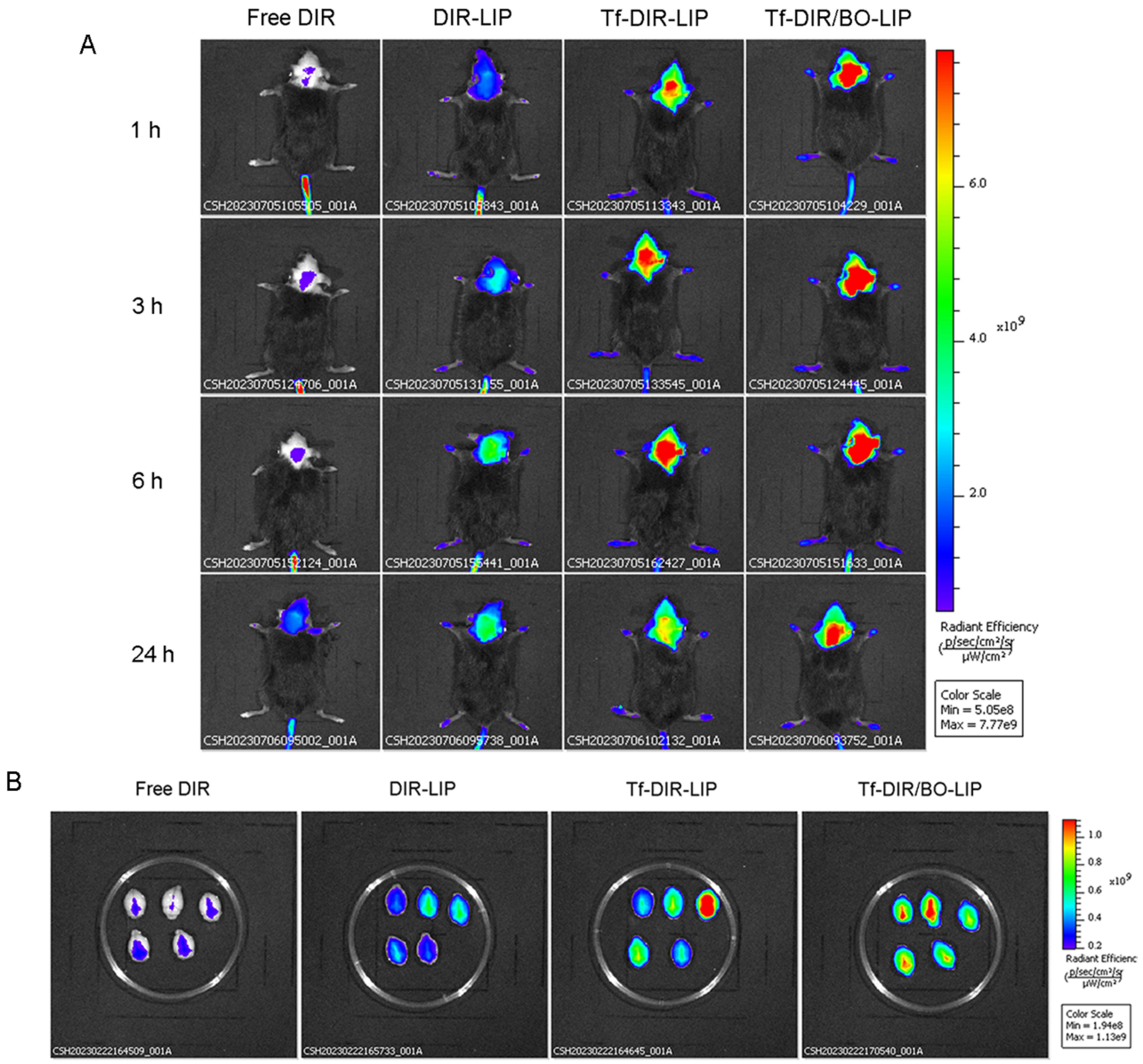

Figure 5 Evaluation of brain targeting characteristics and in vivo. (**A**) Real-time imaging observation after intravenous administration of varying liposomal formulations in TBI mice (n=3). (**B**) Fluorescence images of brain tissues in TBI mice at 24 hours after administration of DIR-Lip, Tf-DIR-Lip and Tf-DIR/BO-Lip (n=5).

targeted approach ensures higher concentrations of rapamycin are delivered directly to the site of injury, maximizing therapeutic efficacy. On the other hand, Borneol, incorporated alongside rapamycin in our liposomes, plays a critical role in temporarily disrupting the BBB. This terpene compound facilitates the transcellular pathway, thereby allowing larger molecules, such as those of the liposomes, to penetrate the BBB more effectively. This disruption is hypothesized to occur through borneol's interaction with membrane lipids, altering the lipid organization and increasing membrane fluidity.This synergistic effect with transferrin modification significantly increases the bioavailability of rapamycin in the brain tissue, crucial for addressing the localized inflammation and neuronal damage post-TBI.

The Protective Effect of TF-RAPA/BO-LIP in TBI Mice

To evaluate the potential neuroprotective effects of TF-RAPA/BO-LIP following TBI, we utilized the NSS to assess neurological function 24 hours after TBI induction. As depicted in Figure 6A, the NSS score significantly increased in the TBI group compared to the Sham group, confirming successful TBI modeling.Notably, all rapamycin formulation

https://doi.org/10.2147/IJN.S489165

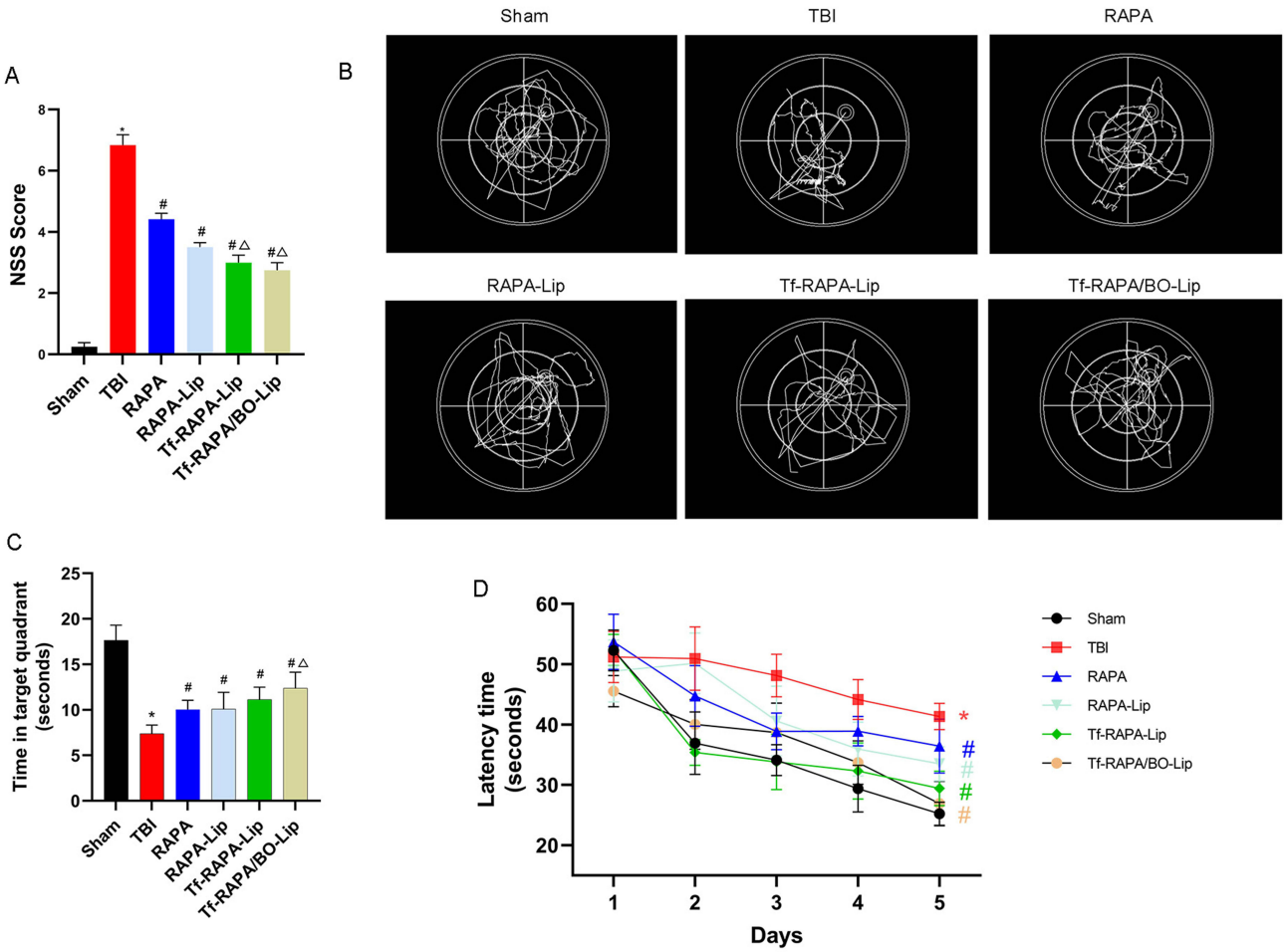

Figure 6 Different formulations of rapamycin reduces neurological damage, and cognitive dysfunction after TBI. (**A**) Degree of neurological impairment represented by NSS scores. (**B**) Representative swimming trace for each group in the probe test. (**C**) Duration of stay in the correct quadrant for 1 min in the probe test with the platform removed of the MWM tests. (**D**) Time spent finding the platform in the five days of the MWM tests. The sham group compared with the other groups, **P*<0.05; the TBI group compared with the other groups, $^{\#}P$<0.05; the RAPA group compared with the other groups, $^{\triangle}P$< 0.05.

groups exhibited a substantial reduction in NSS scores compared to the TBI group alone, indicating that these formulations effectively mitigated neuronal damage. Among them, the TF-RAPA-LIP and TF-RAPA/BO-LIP groups showed a more pronounced decrease in NSS scores than the group receiving unmodified RAPA, highlighting the enhanced neuroprotective effect of Tf-modified liposomes.

The Morris Water Maze (MWM) test was employed to evaluate the impact of Tf-modified liposomes on spatial memory and learning abilities post-TBI. During the navigation test (days 2 to 5), mice in the TBI group took significantly longer to locate the hidden platform compared to the Sham group, indicating impaired spatial learning (Figure 6D). However, from day 4 onwards, the RAPA liposome groups, especially the TF-RAPA/BO-LIP group, demonstrated notably shorter escape latencies, suggesting improved spatial learning capabilities.

On day 6, the platform was removed to assess memory retention. Mice in the TBI group spent considerably less time in the target quadrant than the Sham group, underscoring the memory deficits induced by TBI (Figure 6C). Conversely, mice treated with RAPA formulations, particularly the TF-RAPA/BO-LIP group, spent significantly more time in the target quadrant, indicating enhanced memory function.The representative swim traces (Figure 6B) further illustrated these findings. Mice in the TBI group displayed no particular preference for the target quadrant, whereas those in the TF-RAPA/BO-LIP group showed behavior more similar to the Sham group, effectively navigating towards the previous location of the platform.Overall, these results demonstrate that TF-RAPA/BO-LIP not only mitigates neurological damage more effectively than other RAPA formulations but also significantly improves cognitive impairments after

TBI. It follows that the co-delivery system not only enhances drug delivery efficiency but also synergize the neuroprotective effects of rapamycin with borneol's capabilities. Rapamycin's inhibition of the mTOR pathway reduces neuronal apoptosis and mitigates neuroinflammation, which are pivotal in controlling secondary injury cascades following TBI. Borneol contributes additional neuroprotective effects, including anti-inflammatory and antioxidant actions, which together help preserve cognitive functions and neuronal integrity.

RAPA Attenuates TBI-Induced Oxidative Damage

To evaluate the oxidative stress in mice with TBI, we assessed the levels of superoxide dismutase (SOD) activity and malondialdehyde (MDA) in the cerebral cortex tissue. As illustrated in Figure 7A and B, compared to the Sham group, MDA levels were significantly higher and SOD activity was significantly lower in the TBI group. Conversely, in the RAPA-treated group, MDA levels were significantly reduced and SOD activity was significantly increased compared to the TBI group. These findings suggest that RAPA enhances the antioxidant capacity and reduces oxidative stress in mice with TBI.

RAPA Inhibits Ferroptosis After TBI

To verify whether the therapeutic effect of RAPA on TBI is related to ferroptosis, we tested the expression of the ferroptosis-related proteins GPX4, SLC7A11, SLC3A2, FTH1 and DMT1 in the cortex by Western blotting. As shown in the Figure 7C, compared with the Sham group, the expression of GPX4, FTH1, SLC3A2, and SLC7A11 in the TBI group were significantly reduced, and the expression of DMT1 was significantly increased. Compared with the TBI group, We detected an upward trend in the expression levels of GPX4, FTH1, SLC3A2, and SLC7A11 in the RAPA group and a significant decrease in the levels of DMT1. The expression of GPX4, SLC7A11, DMT1, FTH1, and SLC3A2 in the RAPA group were still significantly different compared to the Sham group. These results indicated that TBI is accompanied by ferroptosis, and that RAPA can ameliorate the expression of ferroptosis-related proteins and inhibit TBI-induced ferroptosis.

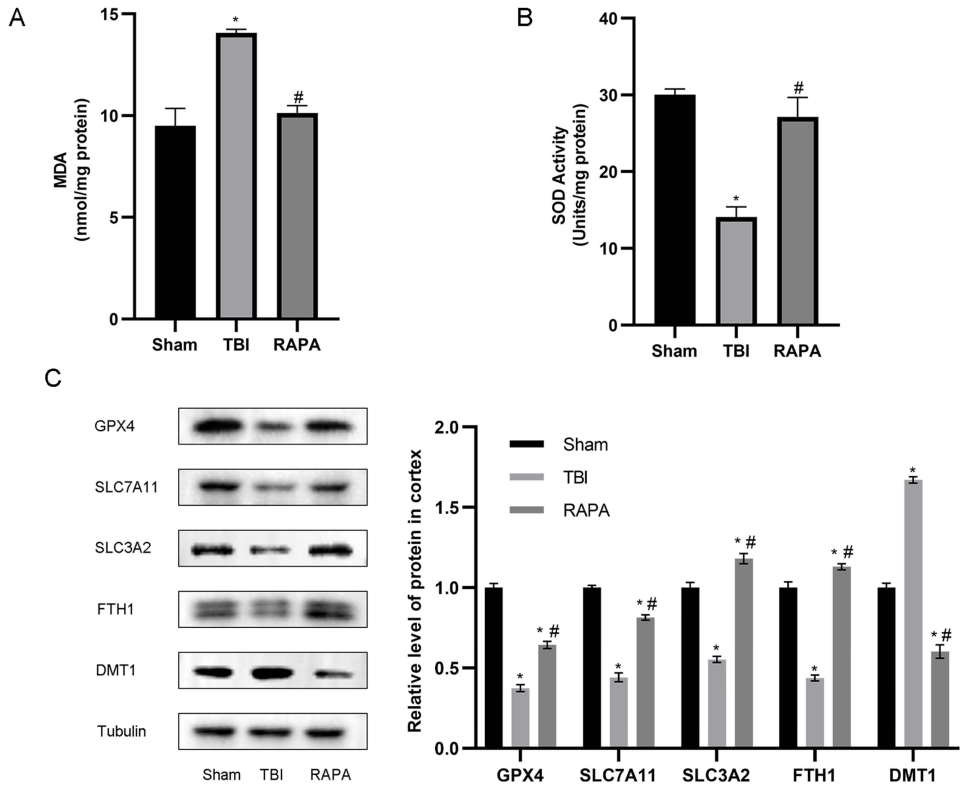

Figure 7 The neuroprotective effect of RAPA on TBI mice. (**A** and **B**) Effect of RAPA on brain oxidative stress. MDA (**A**) and SOD (**B**) levels in cortical tissue homogenate of mice in each group. (**C**) Expression levels of GXP4, SLC7A11, SLC3A2, FTH1 and DMT1 proteins in cortical tissues were detected by Western blot. The Sham group compared with the TBI group or the RAPA group, $^{*}P<0.05$; the TBI group compared with the RAPA group, $^{\#}P<0.05$.

https://doi.org/10.2147/IJN.S489165

Conclusion

In the present study, we developed a brain-targeting nanodelivery system that effectively enhances the permeability of RAPA across the BBB, improving its therapeutic effects on neurological impairments following TBI. This advanced drug delivery vehicle was designed to facilitate the efficient transport of RAPA into the brain using an emulsion-solvent evaporation method. Incorporating transferrin and borneol, the system was optimized to increase drug penetration through targeted delivery.

The results showed that the prepared nanoparticles had a particle size of less than 100 nm, which was suitable for brain-targeted delivery, and demonstrated high encapsulation efficiency exceeding 90%. In addition, Stability assessments confirmed that the liposomes maintained integrity and functionality at 4°C, supporting their potential for long-term storage and use.

In vitro cytological studies indicated that the Tf-modified liposomes significantly enhanced brain uptake via receptor-mediated endocytosis. In vivo evaluations further demonstrated the superior brain-targeting efficiency of these liposomes. The incorporation of borneol was found to increase BBB permeability, allowing for greater accumulation of RAPA in the brain tissue.Pharmacokinetic analyses in vivo highlighted the prolonged circulation and sustained release properties of TF-RAPA/BO-LIP, which are key attributes for achieving lasting therapeutic effects. Behavioral assessments underscored the ability of TF-RAPA/BO-LIP to significantly mitigate cognitive dysfunction post-TBI, indicating its potential as an effective treatment modality.

Our study is among the first to investigate the synergistic mechanism between borneol and transferrin in a liposomal delivery system. The addition of borneol is hypothesized to transiently loosen tight junctions of the BBB, facilitating greater uptake of the transferrin-modified liposomes. The integration of borneol not only facilitates greater drug accumulation within the brain but also contributes to the observed improvements in cognitive functions post-TBI. This dual approach could represent a significant advancement in enhancing drug delivery efficiency compared to systems utilizing either strategy alone.

In conclusion, the engineered liposomes offer a promising strategy for treating neurological impairments post-TBI, marking a significant step forward in the development of effective NDDS. This study lays a foundational basis for further research into the treatment of neurological conditions post-TBI. The enhanced brain accumulation and subsequent neuroprotective effects observed in our TBI model underscore the potential of our approach not only for TBI but also for other neurological conditions where BBB permeability impedes effective drug delivery. This includes neurodegenerative diseases like Alzheimer's and Parkinson's, where effective treatment is often limited by the same barrier. However, the research object of the laboratory animal model cannot fully represent the practical clinical application, and further experimental investigation is needed for validation. While our study provides compelling evidence supporting this innovative delivery system, we recognize the need for further research to precisely delineate borneol's mechanistic contributions and optimize the formulation for potential clinical applications. These future investigations will be crucial for translating our findings into a viable therapeutic option for TBI and potentially other neurological disorders where BBB permeability is a barrier to effective treatment. By addressing these potential challenges, we aim to to realistically pave the way for future research and potential clinical applications.

Funding

This research was supported by Guangzhou Science and Technology Foundation (202201020390), the Science and Technology Project of Guangzhou, Guangzhou Key Laboratory of Precision Medicine for Infectious Diseases (No.2023A03J0813). The authors gratefully acknowledge The Third Affiliated Hospital of Guangzhou Medical University for providing financial support.

Disclosure

Dr Zhengrong Mei reports grants from Guangzhou Science and Technology Foundation, Dr Yanfang Chen reoprts grants from the Science and Technology Project of Guangzhou, Guangzhou Key Laboratory of Precision Medicine for Infectious Diseases, during the conduct of the study. The author(s) report no conflicts of interest in this work.

References

1. Jiang JY, Gao GY, Feng JF. et al. Traumatic brain injury in China. *Lancet Neurol*. 2019;18(3):286–295. doi:10.1016/s1474-4422(18)30469-1
2. Khellaf A, Khan DZ, Helmy A. Recent advances in traumatic brain injury. *J Neurol*. 2019;266(11):2878–2889. doi:10.1007/s00415-019-09541-4
3. Kundu S, Singh S. What Happens in TBI? A Wide Talk on Animal Models and Future Perspective. *Curr Neuropharmacol*. 2023;21(5):1139–1164. doi:10.2174/1570159x20666220706094248
4. Shin MK, Vázquez-Rosa E, Koh Y, et al. Reducing acetylated tau is neuroprotective in brain injury. *Cell*. 2021;184(10):2715–2732.e23. doi:10.1016/j.cell.2021.03.032
5. Dey A, Ghosh S, Bhuniya T, et al. Clinical Theragnostic Signature of Extracellular Vesicles in Traumatic Brain Injury (TBI). *ACS Chem Neurosci*. 2023;14(17):2981–2994. doi:10.1021/acschemneuro.3c00386
6. Harper MM, Rudd D, Meyer KJ, et al. Identification of chronic brain protein changes and protein targets of serum auto-antibodies after blast-mediated traumatic brain injury. *Heliyon*. 2020;6(2):e03374. doi:10.1016/j.heliyon.2020.e03374
7. Kim G, Gautier O, Tassoni-Tsuchida E, Ma XR, Gitler AD. ALS Genetics: gains, Losses, and Implications for Future Therapies. *Neuron*. 2020;108(5):822–842. doi:10.1016/j.neuron.2020.08.022
8. Iacono D, Raiciulescu S, Olsen C, Perl DP. Traumatic Brain Injury Exposure Lowers Age of Cognitive Decline in AD and Non-AD Conditions. *Front Neurol*. 2021;12:573401. doi:10.3389/fneur.2021.573401
9. Dixon KJ. Pathophysiology of Traumatic Brain Injury. *Phys Med Rehab Clin N Am*. 2017;28(2):215–225. doi:10.1016/j.pmr.2016.12.001
10. Pavlovic D, Pekic S, Stojanovic M, Popovic V. Traumatic brain injury: neuropathological, neurocognitive and neurobehavioral sequelae. *Pituitary*. 2019;22(3):270–282. doi:10.1007/s11102-019-00957-9
11. Alouani AT, Elfouly T. Traumatic Brain Injury (TBI) Detection: past, Present, and Future. *Biomedicines*. 2022;10(10):2472. doi:10.3390/biomedicines10102472
12. McConnell HL, Mishra A. Cells of the Blood-Brain Barrier: an Overview of the Neurovascular Unit in Health and Disease. *Methods mol Biol*. 2022;2492:3–24. doi:10.1007/978-1-0716-2289-6_1
13. Mannix R, Berkner J, Mei Z, et al. Adolescent Mice Demonstrate a Distinct Pattern of Injury after Repetitive Mild Traumatic Brain Injury. *J Neurotrauma*. 2017;34(2):495–504. doi:10.1089/neu.2016.4457
14. Butler CR, Boychuk JA, Smith BN. Differential effects of rapamycin treatment on tonic and phasic GABAergic inhibition in dentate granule cells after focal brain injury in mice. *Exp Neurol*. 2016;280:30–40. doi:10.1016/j.expneurol.2016.03.022
15. Haeri A, Osouli M, Bayat F, Alavi S, Dadashzadeh S. Nanomedicine approaches for sirolimus delivery: a review of pharmaceutical properties and preclinical studies. *Artif Cells Nanomed Biotechnol*. 2018;46(sup1):1–14. doi:10.1080/21691401.2017.1408123
16. Blanco E, Sangai T, Wu S, et al. Colocalized delivery of rapamycin and paclitaxel to tumors enhances synergistic targeting of the PI3K/Akt/mTOR pathway. *Mol Ther*. 2014;22(7):1310–1319. doi:10.1038/mt.2014.27
17. Schurhoff N, Toborek M. Circadian rhythms in the blood-brain barrier: impact on neurological disorders and stress responses. *Molecular Brain*. 2023;16(1):5. doi:10.1186/s13041-023-00997-0
18. Khonsari F, Heydari M, Dinarvand R, Sharifzadeh M, Atyabi F. Brain targeted delivery of rapamycin using transferrin decorated nanostructured lipid carriers. *BioImpacts*. 2022;12(1):21–32. doi:10.34172/bi.2021.23389
19. Gupta MN, Roy I. How Corona Formation Impacts Nanomaterials as Drug Carriers. *Mol Pharmaceut*. 2020;17(3):725–737. doi:10.1021/acs.molpharmaceut.9b01111
20. Tang S, Wang A, Yan X, et al. Brain-targeted intranasal delivery of dopamine with borneol and lactoferrin co-modified nanoparticles for treating Parkinson's disease. *Drug Delivery*. 2019;26(1):700–707. doi:10.1080/10717544.2019.1636420
21. William B, Noemie P, Brigitte E, Pjcej G. Supercritical fluid methods: an alternative to conventional methods to prepare liposomes. *Chem Eng J*. 2020;383:123106. doi:10.1016/j.cej.2019.123106
22. Liu X, Meng HJV. Consideration for the scale-up manufacture of nanotherapeutics—A critical step for technology transfer. *View*. 2021;2(5):20200190. doi:10.1002/VIW.20200190
23. Wei T, Cheng Q, Min YL, Olson EN, Siegwart DJ. Systemic nanoparticle delivery of CRISPR-Cas9 ribonucleoproteins for effective tissue specific genome editing. *Nat Commun*. 2020;11(1):3232. doi:10.1038/s41467-020-17029-3
24. Hirunagi T, Sahashi K, Tachikawa K, et al. Selective suppression of polyglutamine-expanded protein by lipid nanoparticle-delivered siRNA targeting CAG expansions in the mouse CNS. *mol Ther Nucleic Acids*. 2021;24:1–10. doi:10.1016/j.omtn.2021.02.007
25. Ma F, Yang L, Sun Z, et al. Neurotransmitter-derived lipidoids (NT-lipidoids) for enhanced brain delivery through intravenous injection. *Sci Adv*. 2020;6(30):eabb4429. doi:10.1126/sciadv.abb4429
26. Rosenblum D, Gutkin A, Kedmi R, et al. CRISPR-Cas9 genome editing using targeted lipid nanoparticles for cancer therapy. *Sci Adv*. 2020;6(47):9450. doi:10.1126/sciadv.abc9450
27. Xiao W, Wang Y, Zhang H, et al. The protein Corona hampers the transcytosis of transferrin-modified nanoparticles through blood-brain barrier and attenuates their targeting ability to brain tumor. *Biomaterials*. 2021;274:120888. doi:10.1016/j.biomaterials.2021.120888
28. Tenchov R, Bird R, Curtze AE, Zhou Q. Lipid Nanoparticles─From Liposomes to mRNA Vaccine Delivery, a Landscape of Research Diversity and Advancement. *ACS nano*. 2021;15(11):16982–17015. doi:10.1021/acsnano.1c04996
29. Wang Y, Yang Y, Yu Y, et al. Transferrin Modified Dioscin Loaded PEGylated Liposomes: characterization and In Vitro Antitumor Effect. *J Nanosci Nanotechnol*. 2020;20(3):1321–1331. doi:10.1166/jnn.2020.16955
30. Sela M, Poley M, Mora-Raimundo P, et al. Brain-Targeted Liposomes Loaded with Monoclonal Antibodies Reduce Alpha-Synuclein Aggregation and Improve Behavioral Symptoms in Parkinson's Disease. *Adv Mater*. 2023;35(51):e2304654. doi:10.1002/adma.202304654
31. Dos Santos Rodrigues B, Arora S, Kanekiyo T, Singh J. Efficient neuronal targeting and transfection using RVG and transferrin-conjugated liposomes. *Brain Res*. 2020;1734:146738. doi:10.1016/j.brainres.2020.146738
32. AlSawaftah NM, Awad NS, Paul V, Kawak PS, Al-Sayah MH, Husseini GA. Transferrin-modified liposomes triggered with ultrasound to treat HeLa cells. *Sci Rep*. 2021;11(1):11589. doi:10.1038/s41598-021-90349-6
33. Stocki P, Szary J, Rasmussen CLM, et al. Blood-brain barrier transport using a high affinity, brain-selective VNAR antibody targeting transferrin receptor 1. *FASEB J*. 2021;35(2):e21172. doi:10.1096/fj.202001787R
34. Willson J. Transferrin' across the blood-brain barrier. *Nat Rev Drug Discov*. 2020;19(7):444. doi:10.1038/d41573-020-00102-3

35. Olsman M, Sereti V, Mühlenpfordt M, et al. Focused Ultrasound and Microbubble Treatment Increases Delivery of Transferrin Receptor-Targeting Liposomes to the Brain. *Ultrasound Med Biol*. 2021;47(5):1343–1355. doi:10.1016/j.ultrasmedbio.2021.01.014
36. Kusmierz CD, Callmann CE, Kudruk S, Distler ME, Mirkin CA. Transferrin Aptamers Increase the In Vivo Blood-Brain Barrier Targeting of Protein Spherical Nucleic Acids. *Bioconjugate Chem*. 2022;33(10):1803–1810. doi:10.1021/acs.bioconjchem.2c00389
37. Wang X, Zhao Y, Dong S, et al. Cell-Penetrating Peptide and Transferrin Co-Modified Liposomes for Targeted Therapy of Glioma. *Molecules*. 2019;24(19):3540. doi:10.3390/molecules24193540
38. Kong L, Li XT, Ni YN, et al. Transferrin-Modified Osthole PEGylated Liposomes Travel the Blood-Brain Barrier and Mitigate Alzheimer's Disease-Related Pathology in APP/PS-1 Mice. *Int j Nanomed*. 2020;15:2841–2858. doi:10.2147/ijn.S239608
39. Kawak P, Sawaftah NMA, Pitt WG, Husseini GA. Transferrin-Targeted Liposomes in Glioblastoma Therapy: a Review. *Int J mol Sci*. 2023;24 (17):13262. doi:10.3390/ijms241713262
40. Dasgupta A, Sun T, Rama E, et al. Transferrin Receptor-Targeted Nonspherical Microbubbles for Blood-Brain Barrier Sonopermeation. *Adv Mater*. 2023;35(52):e2308150. doi:10.1002/adma.202308150
41. Wu T, Zhang A, Lu H, Cheng Q. The Role and Mechanism of Borneol to Open the Blood-Brain Barrier. *Integr Cancer Ther*. 2018;17(3):806–812. doi:10.1177/1534735418767553
42. Tan X, Zhang K, Shi W, Tang Z. Research progress on the regulation and mechanism of borneol on the blood-brain barrier in pathological states: a narrative review focused on ischemic stroke and cerebral glioma. *Transl Cancer Res*. 2023;12(11):3198–3209. doi:10.21037/tcr-23-1487
43. Huang Y, Zhang X, Zhang C, et al. Edaravone Dexborneol Downregulates Neutrophil Extracellular Trap Expression and Ameliorates Blood-Brain Barrier Permeability in Acute Ischemic Stroke. *Mediators Inflamm*. 2022;2022:3855698. doi:10.1155/2022/3855698
44. Zhang Y, Long Y, Yu S, et al. Natural volatile oils derived from herbal medicines: a promising therapy way for treating depressive disorder. *Pharmacol Res*. 2021;164:105376. doi:10.1016/j.phrs.2020.105376
45. Zhang Y, Liu S, Wan J, et al. Preparation, Characterization and in vivo Study of Borneol-Baicalin-Liposomes for Treatment of Cerebral Ischemia-Reperfusion Injury. *Int j Nanomed*. 2020;15:5977–5989. doi:10.2147/ijn.S259938
46. Yu B, Yao Y, Zhang X, et al. Synergic Neuroprotection Between Ligusticum Chuanxiong Hort and Borneol Against Ischemic Stroke by Neurogenesis via Modulating Reactive Astrogliosis and Maintaining the Blood-Brain Barrier. *Front Pharmacol*. 2021;12:666790. doi:10.3389/fphar.2021.666790
47. Long Y, Liu S, Wan J, et al. Brain targeted borneol-baicalin liposome improves blood-brain barrier integrity after cerebral ischemia-reperfusion injury via inhibiting HIF-1α/VEGF/eNOS/NO signal pathway. *Biomed Pharmacother*. 2023;160:114240. doi:10.1016/j.biopha.2023.114240
48. Lin JF, Liu YS, Huang YC, et al. Borneol and Tetrandrine Modulate the Blood-Brain Barrier and Blood-Tumor Barrier to Improve the Therapeutic Efficacy of 5-Fluorouracil in Brain Metastasis. *Integrat Cancer Therap*. 2022;21:15347354221077682. doi:10.1177/15347354221077682
49. Yarnell AM, Barry ES, Mountney A, Shear D, Tortella F, Grunberg NE. The Revised Neurobehavioral Severity Scale (NSS-R) for Rodents. *Curr Protocols Neurosci*. 2016;75(1):9.52.1–9.52.16. doi:10.1002/cpns.10
50. Sonavane G, Tomoda K, Makino K. Biodistribution of colloidal gold nanoparticles after intravenous administration: effect of particle size. *Colloids Surf B*. 2008;66(2):274–280. doi:10.1016/j.colsurfb.2008.07.004
51. Kulkarni SA, Feng SS. Effects of particle size and surface modification on cellular uptake and biodistribution of polymeric nanoparticles for drug delivery. *Pharm Res*. 2013;30(10):2512–2522. doi:10.1007/s11095-012-0958-3
52. Ribovski L, Hamelmann NM, Paulusse JMJ. Polymeric Nanoparticles Properties and Brain Delivery. *Pharmaceutics*. 2021;13(12):2045. doi:10.3390/pharmaceutics13122045
53. Chen Y, Meng J, Xu Q, et al. Rapamycin improves the neuroprotection effect of inhibition of NLRP3 inflammasome activation after TBI. *Brain Res*. 2019;1710:163–172. doi:10.1016/j.brainres.2019.01.005